



Cite this: *RSC Adv.*, 2023, **13**, 19412

Ionic liquid mixtures as energy storage materials: a preliminary and comparative study based on thermal storage density†

Julio I. Urzúa, ^a María Luisa Valenzuela,^b Jenifer Cavieres^c and María José Inestrosa-Izurieta^a

Fifteen equimolar binary mixtures are synthesized and thermophysically evaluated in this study. These mixtures are derived from six ionic liquids (ILs) based on methylimidazolium and 2,3-dimethylimidazolium cations with butyl chains. The objective is to compare and elucidate the impact of small structural changes on the thermal properties. The preliminary results are compared to previously obtained results with mixtures containing longer eight-carbon chains. The study demonstrates that certain mixtures exhibit an increase in their heat capacity. Additionally, due to their higher densities, these mixtures achieve a thermal storage density equivalent to that of mixtures with longer chains. Moreover, their thermal storage density surpasses that of some conventional materials commonly used for energy storage.

Received 2nd May 2023

Accepted 19th June 2023

DOI: 10.1039/d3ra02901h

rsc.li/rsc-advances

Introduction

Over the years, the search for new materials for energy storage and conversion has driven the evolution of renewable energy technologies. Various types of energy storage technologies play an important role in the efficient integration of renewable energy sources and energy demand management.

These storage technologies encompass various categories, each relying on different mechanisms.^{1–3} Chemical storage involves energy conversion through chemical reactions, exemplified by fuel cells, lithium-ion and post-lithium batteries.^{4–6} Mechanical storage harnesses energy using mechanisms like flywheels and air compression.^{7,8} Electrochemical storage utilizes supercapacitors or electrochemical capacitors to store energy as electrical charge.^{9,10} And finally, thermal storage uses heat for later use, by heating materials such as molten salts or water, or by storing latent heat in phase-change materials.

This latest technology has aroused great scientific and technological interest due to its simple and practical application. When applied on an industrial scale, known as concentrating solar power (CSP), it demonstrates an impressive ability

to generate electricity from solar energy. CSP power plants consist of numerous solar collector mirrors that redirect the sun's rays to a specific area. Within this zone, a heat transfer fluid (HTF) is stored or housed in a thermal energy storage (TES) system.^{11–14}

Nitrate salts (40% KNO_3 + 60% NaNO_3), eutectic mixture of diphenyl (DPO) and biphenyl oxide (Therminol VP-1), and mineral or silicone oil are the most commonly used materials as HTF and TES in CSP solar plants. However, each has aspects that hinder the efficiency of the process. For example, nitrated salts have a high melting point, which requires high temperatures, and run the risk of solidification in cold weather; additionally, they generate a high degree of corrosion. Therminol VP-1 has a high vapor pressure at high temperature, which could be harmful to pipelines and increase the risk of ignition; mineral oils and silicones, on the other hand, have a limited working range since they decompose at low temperatures.¹⁵ In view of the above, the development of new storage materials is key. In this context, ionic liquids (ILs) are materials that have been proposed in a wide range of applications,¹⁶ and their use as heat transfer and thermal storage fluids has been proposed based on their unique properties, such as low vapor pressure, non-flammability, chemical and thermal stability, and a wide temperature range in the liquid state, properties that offer significant advantages over molten salts and thermal oils.

Considerable studies indicate that methylimidazolium-based ionic liquids exhibit interesting thermal properties; however, many of them do not outperform the thermal properties of conventional materials, such as thermal storage density, a key property in HTF and TES that relates density (ρ), heat capacity (C_p), and operating temperature. This has

^aCentro de Materiales para la Transición y Sostenibilidad Energética, Comisión Chilena de Energía Nuclear, Ruta 68, km 20, Pudahuel, Santiago, Chile. E-mail: julio.urzua@ccchen.cl

^bUniversidad Autónoma de Chile, Facultad de Ingeniería, Instituto de Ciencias Químicas Aplicadas, Grupo de Investigación en Energía y Procesos Sustentables, Av. El Llano Subercaseaux 2801, Santiago, Chile

^cDepartamento de Ingeniería Química y Ambiental, Universidad Técnica Federico Santa María, Av. Vicuña Mackenna 3939, San Joaquín, Santiago, Chile

† Electronic supplementary information (ESI) available. See DOI: <https://doi.org/10.1039/d3ra02901h>



Table 1 Six initial ionic liquids

No.	Compound	Abbreviation	State at r.t.
IL1	1-Butyl-3-methylimidazolium tetrafluoroborate	[Bmim][BF ₄]	Liquid
IL2	1-Butyl-3-methylimidazolium hexafluorophosphate	[Bmim][PF ₆]	Liquid
IL3	1-Butyl-3-methylimidazolium bis(trifluoromethyl sulfonyl) imide	[Bmim][Tf ₂ N]	Liquid
IL4	1-Butyl-2,3-dimethylimidazolium tetrafluoroborate	[Bdmim][BF ₄]	Liquid
IL5	1-Butyl-2,3-dimethylimidazolium hexafluorophosphate	[Bdmim][PF ₆]	Solid
IL6	1-Butyl-2,3-dimethylimidazolium bis(trifluoromethyl sulfonyl)imide	[Bdmim][Tf ₂ N]	Liquid

prompted to explore the properties of ionic liquid mixtures, where systems formed by coulombic, van der Waals, and hydrogen bonding interactions of more than two types of ions are considered as an alternative to improve thermal properties.^{17,18}

In addition to the studies performed by other researchers evaluating the thermophysical properties of ionic liquid mixtures,^{19–23} our group has previously demonstrated that certain binary mixtures of ionic liquids based on 1-octyl-3-methylimidazolium and 1-octyl-2,3-dimethyl imidazolium increased their heat capacity and, therefore, their thermal storage density, which allowed preliminary comparison with materials conventionally used in solar energy storage.²⁴

In order to explore the behaviour of mixtures of similar ILs, with small structural differences, and to compare their properties with previously reported mixtures and conventional materials, in this work we carried out the synthesis and thermophysical characterization of six ionic liquids with butyl chains (Table 1), and their equimolar mixtures, in attempt to determine the variation of their properties from those previously defined by the pure components and, in turn, to evaluate these new compounds as potential heat transfer fluids.

Results and discussion

Density

The density of the ILs and mixtures was measured at atmospheric pressure in the temperature range from 293.15 to 355.15 K. In the case of [Bdmim][PF₆], which is solid at room temperature, the density was heated and measured starting at 313.15 K to ensure its liquid state. The values were fitted with the polynomial eqn (1) and the fitting parameters A_0 , A_1 and A_2 for temperatures T in K can be found in the ESI.†

$$\rho = A_0 + A_1 T + A_2 T^2 \quad (1)$$

As reported in the literature on ILs,^{25,26} the density of mixtures and ILs decreases with increasing temperature. In order to compare the results obtained, the density values at 373 K are shown in Table 2. The density values obtained for the mixtures, in most cases, correspond to average values of the densities of their pure components. The measured density range for all species is from 1137.5 kg m⁻³ for [Bdmim][BF₄] to 1354.9 kg m⁻³ corresponding to mixture 9 [Bmim][Tf₂N] + [Bdmim][Tf₂N], in this case slightly increasing the density respect to the pure systems.

On the other hand, the mixtures previously obtained with longer alkyl chains (Octyl) have a range of densities from 1059.8 kg m⁻³ of [Omim][BF₄] to 1255.1 kg m⁻³ of the [Omim][Tf₂N] + [Odmim][Tf₂N] mixtures. The variation in density values is in agreement with that reported in the literature²⁷ regarding the increase in density with decreasing chain length of imidazolium cation-based ionic liquids.

Thermal stability

Thermal stability of ILs and their mixtures was measured by TGA (DTA), and onset decomposition temperature (T_{onset}) data are shown in Table 3. Thermogravimetric analysis graphs are available in the ESI.†

In some cases, the properties of the mixtures can be simply deduced from the neat systems, as is the case for density, but in others the interactions do not show the ideally expected behaviour. Most of the time, the thermal properties must be understood by studying the intermolecular interactions and charge distribution of the ionic liquids.

Table 2 Density of ILs and mixtures at 373 K (ρ (kg m⁻³))

No.	IL	Density
IL1	[Bmim][BF ₄]	1143.7
IL2	[Bmim][PF ₆]	1301.2
IL3	[Bmim][Tf ₂ N]	1350.6
IL4	[Bdmim][BF ₄]	1137.5
IL5	[Bdmim][PF ₆]	1282.2
IL6	[Bdmim][Tf ₂ N]	1340.5

No.	Mixture	Density
M1	[Bmim][BF ₄] + [Bmim][Tf ₂ N]	1287.4
M2	[Bmim][BF ₄] + [Bmim][PF ₆]	1235.8
M3	[Bmim][PF ₆] + [Bmim][Tf ₂ N]	1332.9
M4	[Bdmim][BF ₄] + [Bdmim][Tf ₂ N]	1268.5
M5	[Bdmim][BF ₄] + [Bdmim][PF ₆]	1211.8
M6	[Bdmim][PF ₆] + [Bdmim][Tf ₂ N]	1316.6
M7	[Bmim][BF ₄] + [Bdmim][BF ₄]	1151.9
M8	[Bmim][PF ₆] + [Bdmim][PF ₆]	1283.6
M9	[Bmim][Tf ₂ N] + [Bdmim][Tf ₂ N]	1354.9
M10	[Bmim][BF ₄] + [Bdmim][PF ₆]	1226.1
M11	[Bmim][BF ₄] + [Bdmim][Tf ₂ N]	1268.3
M12	[Bmim][PF ₆] + [Bdmim][BF ₄]	1215.9
M13	[Bmim][PF ₆] + [Bdmim][Tf ₂ N]	1323.9
M14	[Bmim][Tf ₂ N] + [Bdmim][BF ₄]	1271.6
M15	[Bmim][Tf ₂ N] + [Bdmim][PF ₆]	1326.2



Table 3 T_{onset} and C_p of ILs and mixtures. C_p (KJ kg⁻¹ K⁻¹) T_{onset} (K)

No.	IL	T_{onset}	C_p	No.	Mixture	T_{onset}	C_p	No.	Mixture	T_{onset}	C_p
IL1	[Bmim][BF ₄]	675	1.72	M1	[Bmim][BF ₄] + [Bmim][Tf ₂ N]	663	1.55	M10	[Bmim][BF ₄] + [Bdmim][PF ₆]	658	1.39
IL2	[Bmim][PF ₆]	649	1.61	M2	[Bmim][BF ₄] + [Bmim][PF ₆]	640	1.11	M11	[Bmim][BF ₄] + [Bdmim][Tf ₂ N]	678	2.62
IL3	[Bmim][Tf ₂ N]	704	1.45	M3	[Bmim][PF ₆] + [Bmim][Tf ₂ N]	650	1.37	M12	[Bmim][PF ₆] + [Bdmim][BF ₄]	659	1.80
IL4	[Bdmim][BF ₄]	767	1.81	M4	[Bdmim][BF ₄] + [Bdmim][Tf ₂ N]	685	1.02	M13	[Bmim][PF ₆] + [Bdmim][Tf ₂ N]	669	1.68
IL5	[Bdmim][PF ₆]	656	1.65	M5	[Bdmim][BF ₄] + [Bdmim][PF ₆]	656	1.38	M14	[Bmim][Tf ₂ N] + [Bdmim][BF ₄]	683	2.23
IL6	[Bdmim][Tf ₂ N]	707	1.51	M6	[Bdmim][PF ₆] + [Bdmim][Tf ₂ N]	671	1.36	M15	[Bmim][Tf ₂ N] + [Bdmim][PF ₆]	639	2.13
				M7	[Bmim][BF ₄] + [Bdmim][BF ₄]	652	1.75				
				M8	[Bmim][PF ₆] + [Bdmim][PF ₆]	647	1.50				
				M9	[Bmim][Tf ₂ N] + [Bdmim][Tf ₂ N]	690	1.22				

The six initial ILs have an average decomposition temperature (T_{onset}) ranging between 664 K and 703 K, but the average decomposition temperatures of the mixtures are at lower values with respect to their pure systems, *i.e.*, when two ionic liquids are mixed, their thermal stability decreases.

On the other hand, compared to the values obtained previously with octyl chains, mixtures with shorter chains show slightly lower decomposition values, contrary to those reported in the literature.²⁸

In the case of binary mixtures where two anions or two cations are equal, or in other words, three ions, it is observed in the thermogram DTA as a trend, a single peak of maximum decay is similar to one of the pure ILs. This occurs in mixtures 2, 5, 7, 8, and 9. This could indicate that there is an exchange of ions forming an equilibrium.

In M2 (IL1 + IL2), the thermogram DTA acquires the same thermal behaviour as IL2; in the case of M5 (IL4 + IL6), it behaves like IL4; M7 (IL1 + IL4) like IL4; M8 (IL2 + IL5) like IL5, and M9 (IL3 + IL6) like IL6.

In these cases, there is clearly a dominance of the thermal behaviour of ILs based on 1-butyl-2,3-dimethylimidazolium. This could be due to the influence exerted by the methyl group located at the C(2) position of the imidazolium cation (Fig. 1), since this site represents a predominant site for interionic hydrogen bonding. The C(2)-H bond possesses a slightly acidic nature, being substituted by a methyl, it favours charge distribution by forcing the anion to interact to a greater extent *via* hydrogen bonds with C(4) and C(5).²⁹

This domain can also be observed in M4 (IL4 + IL6) and M6 (IL5 + IL6) where the behaviour of each of the base ILs prevails and two decay peaks are observed. On the other hand, in M1

(IL1 + IL3) and M3 (IL2 + IL3) the behaviour is exclusively due to the influence of the anions.³⁰

In binary reciprocal mixtures, composed of four ions, they also reflect the influence of the methyl group located at the C(2) position of the imidazolium cation, since two peaks corresponding to each of the base ILs are clearly defined. This could be one of the reasons for the higher thermal stability of the 1-alkyl-2,3-dimethyl imidazolium cations,³¹ and unlike other properties measured in reciprocal binary mixtures,³²⁻³⁴ in this study it was observed that within a mixture with four different ions, some prior organization could persist that would give rise to different thermal behaviours, even when there are no stability differences between the ions involved.

In the case of M10 (IL1 + IL5), in the thermogram DTA, two peaks of thermal degradation are clearly and well defined, the first peak being IL1 and the second peak IL5; in the case of M11 (IL1 + IL6), M12 (IL2 + IL4), M13 (IL2 + IL6), M14 (IL3 + IL4), and M15 (IL3 + IL5), all two peaks of thermal degradation in the order described.

Finally, in this study, the TGA analysis shows a high thermal stability of the mixtures, and the average T_{onset} value for all of them is around 662 K.

Heat capacity

Differential scanning calorimetry (DSC) was used to calculate the heat capacities (C_p) of the ILs and their mixtures. The DSC tests were carried out at a rate of 10 K min⁻¹ in a temperature range from 273.15 K to 423.15 K.

C_p was calculated from its definition using the following eqn (2).³⁵

$$C_p = \frac{1}{m} \frac{\partial H}{\partial T_p} = \frac{1}{m} \frac{\partial H}{\partial T} \frac{\partial T}{\partial t_p} = \frac{1}{m} \frac{\Delta P}{\beta} \quad (2)$$

where H represents the enthalpy, m the mass of the sample, ΔP is the absolute value of the heat flux to the sample and β the heating rate, which is described by eqn (3).

$$\beta = \frac{T_t - T_0}{t} \quad (3)$$

where T_0 is the initial temperature and T_t is the temperature at time t .

T_0 fit the heat capacity data, the quadratic polynomial eqn (4) was used. The fitting parameters, correlation factor and other data are available in the ESI.†

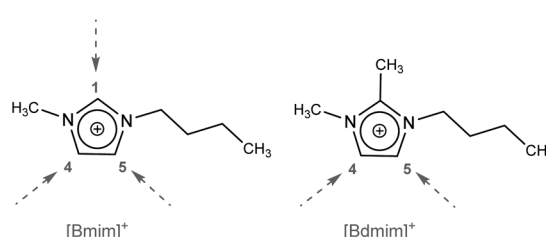


Fig. 1 Structures of imidazolium cations. The dotted arrow indicates the positions of possible hydrogen bonds.



$$C_p = A_0 + A_1 T + A_2 T^2 \quad (4)$$

For comparison, heat capacities data at 373 K are presented in Table 3.

Part of the aim of this study is to corroborate the increase in C_p after mixing two ionic liquids. In the group of mixtures under study, only four of the fifteen mixtures (mixtures 11, 13, 14, and 15) increased their C_p values from neat systems, three of them (1, 7, and 12) showed an intermediate value, and the remaining eight decreased their heat capacity compared to the initial ILs.

Compared to previously reported¹³ values for mixtures with longer alkyl chains, the C_p values are lower, but with an increase reasonably proportional to the basal ionic liquids. A comparison of the C_p values obtained in this study and those obtained previously is shown in Table 4. In addition, the values of the starting ionic liquids are incorporated. In the case of the four mixtures, reported in this work, which increased their C_p values from the neat systems, they are all binary reciprocal mixtures.

There is no structural pattern that can be analysed for each of the mixtures, so the variation in heat capacity is difficult to predict. Ion pairs in an IL are organized into polar and non-polar domains, resulting in structural, transition and relative size segregation of high and low charge regions. These aspects can be influenced by alkyl chain length, and have a direct impact on fluid properties. Thus, the study of intermolecular interactions between anions and cations could give some insight into the molecular behaviour that influences each of the thermophysical properties, with greater interest when studying mixtures, which involve a larger number of ions.

Looking at the cation charges by molecular dynamics, the hydrogen atoms in C(2), C(4), and C(5) apparently carry most of the positive charge, while the negative charge is distributed in N(1) and N(2), as well as between the C(4) and C(5) atoms. Thus, the C(4) and C(5) atoms appear to be almost neutral, whereas the C(2) atom possesses exclusively a positive charge due to electron deficit, which results in higher acidity and a tendency to form strong hydrogen bonds, while, on the contrary, C(4) and C(5) possess electron-donating properties.^{36,37}

The impact of chain length is another aspect to consider. Kasemi *et al.* conducted molecular dynamics simulations to

investigate the influence of chain length in $[C_n\text{mim}][\text{Tf}_2\text{N}]$ ($n = 2, 8$) ionic liquids. Their findings revealed that with a longer alkyl chain ($n = 8$), there is a greater likelihood of locating the C(2)-H groups of the cation and the anionic oxygen atoms within the polar domain. This means that there is a higher probability that hydrogen bonds will form, leading to higher vibrational energy transfer.³⁸ Garaga *et al.*³⁹ showed that, as the alkyl chain length increases, the hydrogen bonds and van der Waals interactions become stronger, while the coulombic strength decreases, and the study of the imidazolium cation and the $[\text{Tf}_2\text{N}]^-$ anion in $[C_n\text{mim}][\text{Tf}_2\text{N}]$ revealed that the overall rotational mobility decreases with n , while different dynamic properties are observed, with the polar domains being the most dynamic and the imidazolium ring and its nearest chain segment being the most rigid. Concluding that the formation of segregated nanodomains in $[C_n\text{mim}][\text{Tf}_2\text{N}]$ is accompanied by the formation of nanodynamic heterogeneities, therefore, the cation slows down its rotational mobility more than the anion, contrary to what is observed for shorter chains.⁴⁰ This reinforces the idea put forward by Rocha *et al.*,⁴¹ who show the increase of the heat capacity in ionic liquids $[C_n\text{mim}][\text{Tf}_2\text{N}]$ as the chain length increases. This analysis could respond to the difference in C_p observed between mixtures with octyl and butyl substituents.

These different analyses could help to understand the heat capacity increase of the mixtures under study from their structures and components. However, for a deeper understanding, it is necessary to further analyse the intermolecular effects as a set because these are complex systems where the binary reciprocal equimolar mixtures differ in their structures and the properties do not follow a deducible pattern.

According to Hunt *et al.*,⁴² the effects caused by the loss of hydrogen bonds could be compensated by the loss of entropy. The disorder in the system is reduced by the elimination of ion pair conformers that are stable for 1-alkyl-3-methyl imidazolium cations, but not for 1-alkyl-2,3-dimethyl imidazolium cations and an increase in the rotational barrier of the butyl chain, which limits free rotation and facilitates the association of the alkyl chain. This analysis could explain that all the mixtures where C_p increases involve a 1-alkyl-2,3-dimethyl imidazolium cation.

Table 4 Comparison of mixtures that increased C_p from their neat systems

Mixture	C_p IL	C_p	Mixture	C_p IL	C_p
$[\text{Bmim}][\text{BF}_4] + [\text{Bdmim}][\text{Tf}_2\text{N}]$	1.72 1.51	2.62	$[\text{Odmim}][\text{BF}_4] + [\text{Odmim}][\text{Tf}_2\text{N}]$	1.83 1.21	2.01
$[\text{Bmim}][\text{PF}_6] + [\text{Bdmim}][\text{Tf}_2\text{N}]$	1.61 1.51	1.68	$[\text{Odmim}][\text{BF}_4] + [\text{Odmim}][\text{PF}_6]$	1.83 2.61	2.83
$[\text{Bmim}][\text{Tf}_2\text{N}] + [\text{Bdmim}][\text{BF}_4]$	1.45 1.81	2.23	$[\text{Omim}][\text{PF}_6] + [\text{Odmim}][\text{PF}_6]$	1.59 2.61	2.97
$[\text{Bmim}][\text{Tf}_2\text{N}] + [\text{Bdmim}][\text{PF}_6]$	1.45 1.65	2.13	$[\text{Omim}][\text{Tf}_2\text{N}] + [\text{Odmim}][\text{Tf}_2\text{N}]$	1.23 1.21	1.99
			$[\text{Omim}][\text{BF}_4] + [\text{Odmim}][\text{Tf}_2\text{N}]$	1.63 1.21	1.70
			$[\text{Omim}][\text{PF}_6] + [\text{Odmim}][\text{BF}_4]$	1.59 1.83	2.28
			$[\text{Omim}][\text{PF}_6] + [\text{Odmim}][\text{Tf}_2\text{N}]$	1.59 1.21	2.31



Thermal storage density

The heat storage density, E , is an important parameter for quantifying the energy stored by a material in a given volume.

For the calculation of E in mixtures and ILs, eqn (5) is used:^{43,44}

$$E = \rho C_p (T_0 - T_i) \quad (5)$$

where ρ is the density value kg m^{-3} , C_p is the heat capacity in $\text{kJ kg}^{-1} \text{K}^{-1}$, and $T_0 - T_i$ are the outlet and inlet temperature, respectively. For comparison, a difference of 100 K (ΔT) has been used. The thermal storage densities obtained in the mixtures and those of other ionic liquids previously analyzed are compared in Table 5.

In Table 6, it is possible to compare the E values of the four mixtures that increased their C_p in this study *vs.* the mixtures with higher C_p with eight-carbon alkyl chain obtained in a previous report.

The results show the dependence of E on density and C_p , since the $[\text{Omim}][\text{PF}_6] + [\text{Odmim}][\text{PF}_6]$ blend has the highest $C_p = 2.9 \text{ kJ kg}^{-1} \text{K}^{-1}$ and a density of 1116 kg m^{-3} , resulting in $E = 324 \text{ MJ m}^{-3}$, while the mixture $[\text{Bmim}][\text{BF}_4] + [\text{Bdmim}][\text{Tf}_2\text{N}]$

has a lower value of $C_p = 2.6$, but a higher density, 1268 kg m^{-3} , which results in a slightly higher value of E , 330 MJ m^{-3} .

It is necessary to consider the working temperatures to make an objective comparison of the thermal storage density values between the mixtures studied and the conventional materials, these values can be observed in Table 6.

Table 6 also shows that the thermal storage densities of the thermal oils are substantially lower than the mixtures, mainly due to their lower density and heat capacity values.

In comparison to the nitrate salts, there is an interesting relationship because, while the density is higher in the nitrate salts, the mixtures have higher C_p values. These differences could compensate the final E value; however, the working temperature (defined mainly by thermal stability) finally determines higher values for nitrated salts.

It is important to highlight that the results obtained in this article demonstrate high reproducibility. The experiments were conducted independently and repeated in triplicate, ensuring the robustness of the data. The results showed significant consistency, with an average variation of less than 5%. Furthermore, comparisons were made with previous research in the field, and it was found that the results are consistent with the trends reported in the literature.

Table 5 Comparison of thermal storage density of ionic liquids and INFs ($\Delta T = 100 \text{ K}$)

Fluid	Reference	$C_p (\text{kJ kg}^{-1} \text{K}^{-1})$	$\rho (\text{kg m}^{-3})$	$E (\text{MJ m}^{-3})$
$[\text{Bmim}][\text{BF}_4]$	This work	1.7	1143	194
$[\text{Bmim}][\text{PF}_6]$	This work	1.6	1301	208
$[\text{Bmim}][\text{Tf}_2\text{N}]$	This work	1.4	1351	189
$[\text{Bdmim}][\text{BF}_4]$	This work	1.8	1138	205
$[\text{Bdmim}][\text{PF}_6]$	This work	1.6	1282	205
$[\text{Omim}][\text{PF}_6]$	24	1.6	1181	189
$[\text{Odmim}][\text{BF}_4]$	24	1.8	1190	214
$[\text{Odmim}][\text{PF}_6]$	24	2.6	1088	283
$[\text{Omim}][\text{PF}_6] + [\text{Odmim}][\text{PF}_6]$	24	2.9	1116	324
$[\text{Omim}][\text{PF}_6] + [\text{Odmim}][\text{BF}_4]$	24	2.3	1199	276
$[\text{Bmim}][\text{BF}_4] + [\text{Bdmim}][\text{Tf}_2\text{N}]$	This work	2.6	1268	330
$[\text{Bmim}][\text{PF}_6] + [\text{Bdmim}][\text{Tf}_2\text{N}]$	This work	1.7	1324	225
$[\text{Bmim}][\text{Tf}_2\text{N}] + [\text{Bdmim}][\text{BF}_4]$	This work	2.2	1272	280
$[\text{Bmim}][\text{Tf}_2\text{N}] + [\text{Bdmim}][\text{PF}_6]$	This work	2.1	1326	278

Table 6 Comparison of thermal storage density of ionic liquids mixtures and conventional thermal fluids

Fluid	Reference	$\rho (\text{kg m}^{-3})$	$C_p (\text{kJ kg}^{-1} \text{K}^{-1})$	$T (\text{K})$	
				$T_{\text{inlet}} - T_{\text{outlet}}$	$E (\text{MJ m}^{-3})$
Mineral oil	43	770	2.60	473.15 – 573.15	200
Silicone oil	43	900	2.10	573.15 – 673.15	189
Synthetic oil	43	900	2.30	523.15 – 533.15	207
Thermolin VP-1	45	991	1.77	523.15 – 663.15	246
$[\text{Omim}][\text{PF}_6] + [\text{Odmim}][\text{PF}_6]$	24	1116	2.97	523.15 – 663.15	464
$[\text{Omim}][\text{PF}_6] + [\text{Odmim}][\text{BF}_4]$	24	1199	2.28	523.15 – 663.15	383
$[\text{Bmim}][\text{BF}_4] + [\text{Bdmim}][\text{Tf}_2\text{N}]$	This work	1268	2.62	523.15 – 663.15	465
$[\text{Bmim}][\text{Tf}_2\text{N}] + [\text{Bdmim}][\text{BF}_4]$	This work	1272	2.23	523.15 – 663.15	397
Nitrate salts	46	1870	1.54	538.15 – 838.15	864



Experimental

General information

All reagents were used as purchased from commercial sources without further purification. 1-Methylimidazole ($C_4H_6N_2$, Merck Millipore, $\geq 99.0\%$), 1,2-dimethylimidazole ($C_5H_8N_2$, Merck Millipore, $\geq 98.0\%$), 1-bromobutane ($CH_3(CH_2)_3Br$, Sigma Aldrich, 99.0%), potassium hexafluorophosphate (KPF_6 , Sigma Aldrich, $\geq 99.99\%$), bis(trifluoromethane)-sulfonimide lithium salt ($Li[Tf_2N]$ Sigma Aldrich, $\geq 99.95\%$), sodium tetrafluoroborate ($NaBF_4$, Sigma Aldrich, $\geq 98\%$), acetonitrile (CH_3CN , Merck Millipore, $\geq 99.8\%$), acetone (CH_3COCH_3 , EMSURE® Merck Millipore, $\geq 99.8\%$), chloroform (CH_3Cl , EMSURE® Merck Millipore, $\geq 99.8\%$), ethyl acetate ($C_4H_8O_2$, EMSURE, Merck Millipore, $\geq 99.5\%$), dichloromethane (CH_2Cl_2 , EMSURE® Merck Millipore, $\geq 99.8\%$), sodium sulfate anhydrous (Na_2SO_4 , EMSURE® Merck Millipore, $\geq 99.0\%$), diatomaceous earth (Kieselguhr, GR for analysis, Merck Millipore), Milli-Q distilled water was used in all the syntheses.

Experimental information. The six ionic liquids synthesized for this study were obtained following the literature and are described extensively in the ESI.† Briefly, from the reaction of 1-bromobutane and 1-methylimidazole (or 1,2-dimethylimidazole), $[Bmim][Br]$ and $[Bdmim][Br]$ were obtained. Subsequently, ionic liquids were prepared by metathesis reaction of the corresponding bromide with sodium tetrafluoroborate (or potassium hexafluorophosphate, or lithium bis[trifluoromethanesulfonyl]imide).

1H and ^{13}C NMR spectra were recorded on Bruker AMX-400 (11.74 T, 400 MHz to 1H and 126 MHz to ^{13}C) NMR spectrometers using the residual proton or the carbon signal of the deuterated solvent as an internal standard.

Thermogravimetric analysis (TGA-DTA) was conducted using a PerkinElmer TGA400S model, operating at a voltage range of 100–240 V and frequency of 50–60 Hz. The experiments were carried out in the temperature range of 303 K to 873 K, with a flow rate of 50 ml min $^{-1}$ and a heating rate of 10 °C min $^{-1}$. The samples, weighing between 2.5 to 5 mg, were placed in platinum crucibles, and the analysis was performed under a nitrogen atmosphere as an inert gas. The equipment has a temperature uncertainty of ± 1 °C and a mass uncertainty of 0.005%, ensuring accurate and precise measurements during the analysis.

Differential scanning calorimetry (DSC) was carried out using a Mettler Toledo calorimeter (model 822e, USA) at a heating rate of 10 K min $^{-1}$ and 5 to 10 mg samples in aluminum pots under nitrogen as an inert gas. Calibration for temperature and enthalpy measurements was performed using certified indium and zinc standards as a reference, with an uncertainty of ± 0.2 K for temperature measurement and 2% for enthalpy change. As a comparison test, the procedure was applied to the base fluids, and the results were consistent with C_p values previously reported in the literature.

Densities were measured with a densimeter Anton Paar DMA 4500 M with an accuracy of 0.00005 g cm $^{-3}$ and repeatability of 0.00001 g cm $^{-3}$ in the temperature range of 293.15 to 363.15 K.

The water content of ionic liquids was determined in triplicate by Karl-Fischer titration (model 870 KF Titrino Plus,

Metrohm, Switzerland), after drying it at 70 °C under vacuum in the presence of phosphorus pentoxide conditions for 36 h, giving a water content less than 100 ppm.

The mixtures were prepared by combining equimolar amounts of each IL and were stirred for 12 h at room temperature to ensure complete homogeneity. Nine binary mixtures ($[A][X][Y]$ or $[A][B][X]$) and six reciprocal binary mixtures ($[A][B][X][X][Y]$) were obtained, according to the classification of Welton *et al.*⁴⁷

Conclusions

In this work, we have studied the thermophysical properties of fifteen equimolar binary mixtures of ILs based on 1-butyl-3-methyl imidazolium and 1-butyl-2,3-dimethyl imidazolium cations with tetrafluoroborate, hexafluoroborate, and bis(trifluoromethylsulfonyl)imide anions. Density, thermal stability, and heat capacity were investigated in order to calculate and compare the variation in thermal storage density.

While density may be a predictable property, thermal stability and heat capacity depend directly on the intermolecular interactions between cations and anions of the mixtures, and being complex systems, further studies and modeling must be done to understand the variation of their properties.

Compared to a previous report with mixtures consisting of eight-carbon alkyl chains, the mixtures with butyl substituents presented, on average, higher density values, but lower decomposition temperatures and lower heat capacity. Also, unlike the previous mixtures, only four mixtures increased their heat capacity (mixtures 11, 13, 14 and 15), all of them binary reciprocals.

Despite the decrease in C_p and thermal stability, the thermal storage density of mixture 11 ($[Bmim][BF_4]$ + $[Bdmim][Tf_2N]$), was slightly higher than the previous mixture with higher C_p ($[Omim][PF_6]$ + $[Odmm][PF_6]$), mainly due to the relationship with density.

Finally, as with previous mixtures, two mixtures (11 and 14) demonstrated higher thermal storage density than thermal oils used for energy storage, while compared to nitrated salts, the need for increased density or operating temperatures despite higher heat capacity values is evident. Although this study has successfully demonstrated that equimolar mixing of some ionic liquids significantly increases the thermal storage density, further studies are needed to clearly define a possible use as a thermal fluid.

Conflicts of interest

The authors report no conflicts of interest. The authors alone are responsible for the content and writing of this article.

Acknowledgements

This work was supported by resources from the Chilean Nuclear Energy Commission.

References

- W. Wang, B. Yuan, Q. Sun and R. Wennersten, Application of energy storage in integrated energy systems-A solution to



fluctuation and uncertainty of renewable energy, *J. Energy Storage*, 2022, **52**, 104812, DOI: [10.1016/j.est.2022.104812](https://doi.org/10.1016/j.est.2022.104812).

2 G. Sadeghi, Energy storage on demand: Thermal energy storage development, materials, design, and integration challenges, *Energy Storage Mater.*, 2022, **46**, 192–222, DOI: [10.1016/j.ensm.2022.01.017](https://doi.org/10.1016/j.ensm.2022.01.017).

3 M. Jafari, A. Botterud and A. Sakti, Decarbonizing power systems: A critical review of the role of energy storage, *Renewable Sustainable Energy Rev.*, 2022, **158**, 112077, DOI: [10.1016/j.rser.2022.112077](https://doi.org/10.1016/j.rser.2022.112077).

4 A. Dutta, S. Mitra, M. Basak and T. Banerjee, A comprehensive review on batteries and supercapacitors: Development and challenges since their inception, *Energy Storage*, 2023, **5**, e339, DOI: [10.1002/est2.339](https://doi.org/10.1002/est2.339).

5 Y. Liang and Y. Yao, Designing modern aqueous batteries, *Nat. Rev. Mater.*, 2023, **8**, 109–122, DOI: [10.1038/s41578-022-00511-3](https://doi.org/10.1038/s41578-022-00511-3).

6 M. Gandolfo, J. Amici, L. Fagiolari, C. Francia, S. Bodoardo and F. Bella, Designing photocured macromolecular matrices for stable potassium batteries, *Sustainable Mater. Technol.*, 2022, **34**, e00504, DOI: [10.1016/j.susmat.2022.e00504](https://doi.org/10.1016/j.susmat.2022.e00504).

7 E. Bazdar, M. Sameti, F. Nasiri and F. Haghigat, Compressed air energy storage in integrated energy systems: a review, *Renewable Sustainable Energy Rev.*, 2022, **167**, 112701, DOI: [10.1016/j.rser.2022.112701](https://doi.org/10.1016/j.rser.2022.112701).

8 S. Choudhury, Flywheel energy storage systems: a critical review on technologies, applications, and future prospects, *Int. J. Electr. Power Energy Syst.*, 2021, **31**, e13024, DOI: [10.1002/2050-7038.13024](https://doi.org/10.1002/2050-7038.13024).

9 F. Naseri, S. Karimi, E. Farjah and E. Schaltz, Supercapacitor management system: a comprehensive review of modeling, estimation, balancing, and protection techniques, *Renewable Sustainable Energy Rev.*, 2022, **155**, 111913, DOI: [10.1016/j.rser.2021.111913](https://doi.org/10.1016/j.rser.2021.111913).

10 M. Reina, A. Scalia, G. Auxilia, M. Fontana, F. Bella, S. Ferrero and A. Lamberti, Boosting Electric Double Layer Capacitance in Laser-Induced Graphene-Based Supercapacitors, *Adv. Sustainable Syst.*, 2022, **6**, 2100228, DOI: [10.1002/adssu.202100228](https://doi.org/10.1002/adssu.202100228).

11 A. Elkhatat and S. A. Al-Muhtaseb, Combined “Renewable Energy-Thermal Energy Storage (RE-TES)” Systems: A Review, *Energies*, 2023, **16**, 4471, DOI: [10.3390/en16114471](https://doi.org/10.3390/en16114471).

12 M. Imran Khan, F. Asfand and S. G. Al-Ghamdi, Progress in research and technological advancements of commercial concentrated solar thermal power plants, *Sol. Energy*, 2023, **249**, 183–226, DOI: [10.1016/j.solener.2022.10.041](https://doi.org/10.1016/j.solener.2022.10.041).

13 M. Imran Khan, F. Asfand and S. G. Al-Ghamdi, Progress in technology advancements for next generation concentrated solar power using solid particle receivers, *Sustainable Energy Technol. Assess.*, 2022, **54**, 102813, DOI: [10.1016/j.seta.2022.102813](https://doi.org/10.1016/j.seta.2022.102813).

14 A. Palacios, C. Barreneche, M. E. Navarro and Y. Ding, Thermal energy storage technologies for concentrated solar power-a review from a materials perspective, *Renewable Energy*, 2020, **156**, 1244e1265, DOI: [10.1016/j.renene.2019.10.1275](https://doi.org/10.1016/j.renene.2019.10.1275).

15 S. Karella, and T. C. Roumpedakis, in *Solar Hydrogen Production: Processes*, Chapter 7 – Solar thermal power plants, Systems and Technologies, 2019, pp. 179–235, DOI: [10.1016/B978-0-12-814853-2.00007-2](https://doi.org/10.1016/B978-0-12-814853-2.00007-2).

16 E. Kianfar and S. Mafi, Ionic Liquids: Properties, Application, and Synthesis, *Fine Chem. Eng.*, 2020, **2**, 22–31, DOI: [10.37256/fce.212021693](https://doi.org/10.37256/fce.212021693).

17 S. L. Piper, M. Kar, D. R. MacFarlane, K. Matuszek and J. M. Pringle, Ionic liquids for renewable thermal energy storage-a perspective, *Green Chem.*, 2022, **24**, 102–117, DOI: [10.1039/D1GC03420K](https://doi.org/10.1039/D1GC03420K).

18 E. Fabre and S. M. S. Murshed, A review of the thermophysical properties and potential of ionic liquids for thermal applications, *J. Mater. Chem. A*, 2021, **9**, 15861–15879, DOI: [10.1039/D1TA03656D](https://doi.org/10.1039/D1TA03656D).

19 S. M. Purcell, P. D. Lane, L. D'Andrea, N. S. Elstone, D. W. Bruce, J. M. Slattery, E. J. Smoll Jr, S. J. Greaves, M. L. Costen, T. K. Minton and K. G. McKendrick, Surface Structure of Alkyl/Fluoroalkylimidazolium Ionic-Liquid Mixtures, *J. Phys. Chem. B*, 2022, **126**, 1962–1979, DOI: [10.1021/acs.jpcb.1c10460](https://doi.org/10.1021/acs.jpcb.1c10460).

20 K. D. Amirchand and V. Singh, Density, speed of sound, and surface tension of binary aqueous solutions containing ammonium based protic ionic liquids, *J. Mol. Liq.*, 2022, **354**, 118845, DOI: [10.1016/j.molliq.2022.118845](https://doi.org/10.1016/j.molliq.2022.118845).

21 B. Golub, D. Ondo, V. Overbeck, R. Ludwig and D. Paschek, Hydrogen bond redistribution effects in mixtures of protic ionic liquids sharing the same cation: non-ideal mixing with large negative mixing enthalpies, *Phys. Chem. Chem. Phys.*, 2022, **24**, 14740–14750, DOI: [10.1039/D2CP01209J](https://doi.org/10.1039/D2CP01209J).

22 Q. Liu, L. Ma, S. Wang, Z. Ni, X. Fu, J. Wang and Q. Zheng, Study on the properties of density, viscosity, excess molar volume, and viscosity deviation of [C2mim][NTf₂], [C2mmim][NTf₂], [C4mim][NTf₂], and [C4mmim][NTf₂] with PC binary mixtures, *J. Mol. Liq.*, 2021, **325**, 114573, DOI: [10.1016/j.molliq.2020.114573](https://doi.org/10.1016/j.molliq.2020.114573).

23 T.-M. Chang and S. E. Billeck, Structure, Molecular Interactions, and Dynamics of Aqueous [BMIM][BF₄] Mixtures: A Molecular Dynamics Study, *J. Phys. Chem. B*, 2021, **125**, 1227–1240, DOI: [10.1021/acs.jpcb.0c09731](https://doi.org/10.1021/acs.jpcb.0c09731).

24 S. Mora, G. Neculqueo, R. A. Tapia and J. I. Urzúa, Thermal storage density of ionic liquid mixtures: a preliminary study as thermal fluid, *J. Mol. Liq.*, 2019, **282**, 221–225, DOI: [10.1016/j.molliq.2019.02.124](https://doi.org/10.1016/j.molliq.2019.02.124).

25 T. C. Paul, A. Tikadar, R. Mahmud, A. S. Salman, A. M. Morshed and J. A. Khan, A Critical Review on the Development of Ionic Liquids-Based Nanofluids as Heat Transfer Fluids for Solar Thermal Energy, *Processes*, 2021, **9**, 858, DOI: [10.3390/pr9050858](https://doi.org/10.3390/pr9050858).

26 A. F. Bouarab, J.-P. Harvey and C. Robelin, Viscosity models for ionic liquids and their mixtures, *Phys. Chem. Chem. Phys.*, 2021, **23**, 733–752, DOI: [10.1039/D0CP05787H](https://doi.org/10.1039/D0CP05787H).

27 E. A. Chernikova, L. M. Glukhov, V. G. Krasovskiy, L. M. Kustov, M. G. Vorobyeva and A. A. Koroteev, Ionic liquids as heat transfer fluids: comparison with known systems, possible applications, advantages and



disadvantages, *Russ. Chem. Rev.*, 2015, **84**, 875–890, DOI: [10.1070/rctr4510](https://doi.org/10.1070/rctr4510).

28 C. Maton, N. De Vos and C. V. Stevens, Ionic liquid thermal stabilities: decomposition mechanisms and analysis tools, *Chem. Soc. Rev.*, 2013, **42**, 5963–5977, DOI: [10.1039/C3CS60071H](https://doi.org/10.1039/C3CS60071H).

29 B. Haddad, J. Kiefer, H. Brahim, H. Belarbi, D. Villemin, S. Bresson, O. Abbas, M. Rahmouni, A. Paolone and O. Palumbo, Effects of C(2) Methylation on Thermal Behavior and Interionic Interactions in Imidazolium-Based Ionic Liquids with Highly Symmetric Anions, *Appl. Sci.*, 2018, **8**, 1043, DOI: [10.3390/app8071043](https://doi.org/10.3390/app8071043).

30 Y. Liu, X. Chen, S. Men, P. Licence, F. Xi, Z. Ren and W. Zhu, The impact of cation acidity and alkyl substituent on the cation-anion interactions of 1-alkyl-2,3-dimethylimidazolium ionic liquids, *Phys. Chem. Chem. Phys.*, 2019, **21**, 11058–11065, DOI: [10.1039/C9CP01381D](https://doi.org/10.1039/C9CP01381D).

31 D. M. Fox, W. H. Awad, J. W. Gilman, P. H. Maupin, H. C. De Long and P. C. Trulove, Flammability, thermal stability, and phase change characteristics of several trialkylimidazolium salts, *Green Chem.*, 2003, **5**, 724–727, DOI: [10.1039/B308444B](https://doi.org/10.1039/B308444B).

32 S. Seki, N. Serizawa, S. Ono, K. Takei, K. Hayamizu, S. Tsuzuki and Y. Umebayashi, Densities, Viscosities, and Refractive Indices of Binary Room-Temperature Ionic Liquids with Common Cations/Anions, *J. Chem. Eng. Data*, 2019, **64**, 433–441, DOI: [10.1021/acs.jced.8b00334](https://doi.org/10.1021/acs.jced.8b00334).

33 M. Kunze, S. Jeong, E. Paillard, M. Winter and S. Passerini, Melting Behavior of Pyrrolidinium-Based Ionic Liquids and Their Binary Mixtures, *J. Phys. Chem. C*, 2010, **114**, 12364–12369, DOI: [10.1021/jp103746k](https://doi.org/10.1021/jp103746k).

34 G. Huang, W.-C. Lin, P. He, Y. Pan and C.-M. Shu, Thermal decomposition of imidazolium-based ionic liquid binary mixture: processes and mechanisms, *J. Mol. Liq.*, 2018, **272**, 37–42, DOI: [10.1016/j.molliq.2018.09.058](https://doi.org/10.1016/j.molliq.2018.09.058).

35 M. M. Zhang and R. G. Reddy, Thermodynamic properties of C4mim[Tf2N] ionic liquids, *Miner. Process. Extr. Metall.*, 2010, **6**, 71–76, DOI: [10.1179/037195510X12665949176490](https://doi.org/10.1179/037195510X12665949176490).

36 K. Fumino, T. Peppel, M. Geppert-Rybacznska, D. H. Zaitsau, J. K. Lehmann, S. P. Verevkin, M. Köckerling and R. Ludwig, The influence of hydrogen bonding on the physical properties of ionic liquids, *Phys. Chem. Chem. Phys.*, 2011, **13**, 14064–14075, DOI: [10.1039/C1CP20732F](https://doi.org/10.1039/C1CP20732F).

37 K. Noack, P. S. Schulz, N. Paape, J. Kiefer, P. Wasserscheidb and A. Leipertza, The role of the C2 position in interionic interactions of imidazolium based ionic liquids: a vibrational and NMR spectroscopic study, *Phys. Chem. Chem. Phys.*, 2010, **12**, 14153–14161, DOI: [10.1039/C0CP00486C](https://doi.org/10.1039/C0CP00486C).

38 M. M. Kazemi, M. Namboodiri, P. Donfack, A. Materny, D. Kerlé, B. Rathke and J. Kiefer, Influence of the alkyl side-chain length on the ultrafast vibrational dynamics of 1-alkyl-3-methylimidazolium bis(trifluoromethylsulfonyl) amide (CnmimNTf2) ionic liquids, *Phys. Chem. Chem. Phys.*, 2017, **19**, 15988–15995, DOI: [10.1039/C7CP02686B](https://doi.org/10.1039/C7CP02686B).

39 M. N. Garaga, M. Nayeri and A. Martinelli, Effect of the alkyl chain length in 1-alkyl-3-methylimidazolium ionic liquids on inter-molecular interactions and rotational dynamics: a combined vibrational and NMR spectroscopic study, *J. Mol. Liq.*, 2015, **210**, 169–177, DOI: [10.1016/j.molliq.2015.06.055](https://doi.org/10.1016/j.molliq.2015.06.055).

40 A. Martinelli, M. Marechal, A. Ostlund and J. Cambedouzou, Insights into the interplay between molecular structure and diffusional motion in 1-alkyl-3-methylimidazolium ionic liquids: a combined PFG NMR and X-ray scattering study, *Phys. Chem. Chem. Phys.*, 2013, **15**, 5510–5517, DOI: [10.1039/C3CP00097D](https://doi.org/10.1039/C3CP00097D).

41 M. A. A. Rocha, M. Bastos, J. A. P. Coutinho and L. M. N. B. F. Santos, Heat capacities at 298.15 K of the extended [CnC1im][Ntf2] ionic liquid series, *J. Chem. Thermodyn.*, 2012, **53**, 140–143, DOI: [10.1016/j.jct.2012.04.025](https://doi.org/10.1016/j.jct.2012.04.025).

42 P. A. Hunt, Why does a reduction in hydrogen bonding lead to an increase in viscosity for the 1-butyl-2,3-dimethylimidazolium-based ionic liquids?, *J. Phys. Chem. B*, 2007, **111**, 4844–4853, DOI: [10.1021/jp067182p](https://doi.org/10.1021/jp067182p).

43 M. Zhang and R. Reddy, Application of [C4min][Tf2N] ionic liquid as thermal storage and heat transfer fluids, *ECS Trans.*, 2007, **28**, 27–34, DOI: [10.1149/1.2409040](https://doi.org/10.1149/1.2409040).

44 A. Lamas, I. Brito, F. Salazar and T. A. Gruber, Synthesis and characterization of physical, thermal and thermodynamic properties of ionic liquids based on [C12mim] and [N444H] cations for thermal energy storage, *J. Mol. Liq.*, 2016, **224**, 999–1007, DOI: [10.1016/j.molliq.2016.10.103](https://doi.org/10.1016/j.molliq.2016.10.103).

45 S. Mathew, G. Visavale, and V. Mali, *Conference: International Conference on Applications of Renewable and Sustainable Energy for Industry and Society*, Hyderabad, REIS-2010, DOI: [10.13140/2.1.3247.4241](https://doi.org/10.13140/2.1.3247.4241).

46 M. Zhang and R. Reddy, Application of [C4min][Tf2N] ionic liquid as thermal storage and heat transfer fluids, *ECS Trans.*, 2007, **28**, 27–34, DOI: [10.1149/1.2409040](https://doi.org/10.1149/1.2409040).

47 H. Niedermeyer, J. P. Hallett, I. J. Villar-Garcia, P. A. Hunt and T. Welton, Mixtures of ionic liquids, *Chem. Soc. Rev.*, 2012, **41**, 7780–7802, DOI: [10.1039/C2CS35177C](https://doi.org/10.1039/C2CS35177C).

